Path Following Control of a Planar Snake Robot with an Exponentially Stabilizing Joint Control Law

Ehsan Rezapour* Pål Liljebäck*,**

** Norwegian University of Science and Technology (NTNU), NO-7491 Trondheim, Norway*
*** SINTEF ICT, Dept. of Applied Cybernetics, NO-7465 Trondheim, Norway*
e-mails: Ehsan.Rezapour@itk.ntnu.no, Pal.Liljeback@sintef.no

Abstract: This paper considers the problem of path following control of a planar snake robot without sideslip constraints. We use Lagrangian mechanics to derive the dynamical equations of motion of the system. The possibility of controlling the orientation of the robot in the absence of external dissipative forces is investigated. An exponentially stabilizing joint control law for the actuated shape dynamics of the robot is presented. We analytically design a guidance-based path following control law for the snake robot, and we show that the trajectories of the heading error dynamics are ultimately bounded with a bound that can be made arbitrarily small. The efficiency of the control design is shown with simulations.

Keywords: Ultimate boundedness, Ultimate bound, Exponentially stabilizing joint control law, Snake robot, Biologically inspired robots, Path following.

1. INTRODUCTION

Snake robots are slender hyper-redundant, i.e. have a large degree of kinematic redundancy, robots that have the capability of being used in operations in narrow and unstructured environments, where the traditional types of mobile robots such as wheeled and legged robots might not be usable. Fire-fighting operations, mine detection and elimination, and pipelines inspection are typical areas where snake robots are potentially useful. In particular, the hyper-redundant structure of these robots enables them to keep the mechanical stability even in failure of some their actuators. However, the *underactuated* structure of these robots which is characterized by the lack of direct control of some degrees of freedom (DOF) makes them a challenging control problem.

The earliest contributions on empirical and analytical studies of snake robot locomotion were reported by Gray (1946). Hirose (1993) proposed a mathematical description of the most common form of snake locomotion, i.e. lateral undulation, which is known as the serpenoid curve. Osterowski (1996) used geometric methods to study the basic problems in undulatory robotic locomotion. Saito (2002) found the optimized parameters of the serpenoid curve through simulating a planar snake robot. Ma (2001) used computer simulations to optimize the motion of a wheel-less snake robot. Date *et al.* (2001) developed controllers for wheeled snake robots aimed at minimizing the lateral constraint forces on the wheels of the robot during locomotion. Nilsson (2004) analyzed the planar snake locomotion with isotropic friction based on energy arguments. Transeth *et al.* (2008) and Liljebäck *et al.* (2012) introduced and developed the concept of *obstacle aided locomotion* for motion control of snake robots in cluttered environments. Liljebäck *et al.* (2010) proposed a path following control law for the snake robot, developed through a cascaded systems theory approach, where the control design is based on a simplified model of the robot.

In contrast with the previous works on snake robots, the contribution of this paper is the analytical design of a guidance-based path following control law for the position of the center of mass (CM) of the snake robot to converge to and follow a desired planar path. In particular, the actuated shape variables, i.e. set of variables defining the internal configuration of the robot, are controlled using an exponentially stabilizing joint control law to track a serpentine motion. Furthermore, the underactuated position variables, i.e. orientation and the position of the CM of the robot, are controlled through an analytically designed guidance-based path following control law. Moreover, we use perturbation analysis to show the ultimate boundedness of the solutions of the heading error dynamics.

The organization of the paper is as follows. In Section 2, we present complete kinematic and dynamic models of a planar snake robot without sideslip constraints. In Section 3, we investigate the possibility of reorienting a planar snake robot in the absence of the external dissipative forces. In Section 4, we define the control design objectives. In Section 5, we propose an exponentially stabilizing joint control law for the robot to track a serpentine motion. In Section 6, a guidance-based path following control design is presented. In Section 7, a guidance law which defines the desired heading angle for the robot is defined. Finally, in Section 8, the simulation results for a planar snake robot are presented to show the efficiency of our control design.

2. MODELING

In order to perform control design, we need to write the governing equations of the system in an implementable way. This is often done by choosing a local coordinate chart and writing the equations with respect to (w.r.t.) these coordinates. According to the illustration of the snake robot in Fig.1, we define the vector of the generalized coordinates of the N-link snake robot as $q = \left[q_1, q_2, \dots, q_{N-1}, \bar{\theta}, p_x, p_y\right]^T \in \mathbb{R}^{N+2}$, where q_i with $i \in \{1, \dots, N-1\}$ denotes the relative

joint angle of the i-th link, $\bar{\theta}$ denotes the absolute heading angle of the robot which will be defined below, and the pair (p_x, p_y) describes the position of the CM of the robot w.r.t. the inertial frame. The vector of the generalized velocities is defined as $\dot{q} = \left[\dot{q}_1, \dot{q}_2, \dots, \dot{q}_{N-1}, \dot{\bar{\theta}}, \dot{p}_x, \dot{p}_y\right]^T \in \mathbb{R}^{N+2}$. Using these coordinates, it is possible to specify the kinematic map of the robot.

1.1 The Kinematic Model

Based on the kinematic parameters of the snake robot given in Fig. 1, it is possible to write the coordinate representation of the forward kinematic map. The map between the absolute link angles θ_i and the relative joint angles q_i can be given as

$$\theta_i = \sum_{t=i}^{N-1} q_t + \theta_N \tag{1}$$

The absolute heading angle of the robot $\bar{\theta}$ can be defined as the average of the absolute link angles

$$\bar{\theta} = \frac{1}{N}\sum_{i=1}^{N} \theta_i \tag{2}$$

The position of the CM of the i-th link w.r.t. the global x and y axes can be, respectively, given as

$$\begin{aligned} x_i &= x_0 + 2l\sum_{j=1}^{i-1}\cos\theta_j + l\cos\theta_i \\ y_i &= y_0 + 2l\sum_{j=1}^{i-1}\sin\theta_j + l\sin\theta_i \end{aligned} \tag{3}$$

where $2l$ is the length of a link, and (x_0, y_0) is the tail position, cf. Fig. 1. The linear velocities of the CM of the i-th link w.r.t. the global x and y axes can be found by taking the time-derivative of (3)

$$\begin{aligned} \dot{x}_i &= \dot{x}_0 - 2l\sum_{j=1}^{i-1}\sin\theta_j\dot{\theta}_j - l\sin\theta_i\dot{\theta}_i \\ \dot{y}_i &= \dot{y}_0 + 2l\sum_{j=1}^{i-1}\cos\theta_j\dot{\theta}_j + l\cos\theta_i\dot{\theta}_i \end{aligned} \tag{4}$$

Since all the links have equal length and mass, the position of the CM for the whole structure of the robot is defined as

$$\begin{aligned} p_x &= \frac{1}{N}\sum_{i=1}^{N} x_i \\ p_y &= \frac{1}{N}\sum_{i=1}^{N} y_i \end{aligned} \tag{5}$$

To facilitate path following control of the CM of the snake robot, we replace the tail position (x_0, y_0) in (3) with the position of the CM of the robot (p_x, p_y) using the following change of coordinates

$$\begin{aligned} x_0 &= p_x - \frac{1}{N}\sum_{i=1}^{N}\left(2l\sum_{j=1}^{i-1}\cos\theta_j + l\cos\theta_i\right) \\ y_0 &= p_y - \frac{1}{N}\sum_{i=1}^{N}\left(2l\sum_{j=1}^{i-1}\sin\theta_j + l\sin\theta_i\right) \end{aligned} \tag{6}$$

To write the kinematic map in accordance with the specified generalized coordinates, we write the absolute link angles in terms of the heading and the relative joint angles as

$$\theta_i = \sum_{t=i}^{N-1} q_t + \left(-\frac{1}{N}\sum_{z=1}^{N-1} z q_z + \bar{\theta}\right) \tag{7}$$

Substituting (6)–(7) along with their time-derivatives into (3)-(4) completes the derivation of the kinematic map of the snake robot w.r.t. the specified coordinate chart.

1.2 The Euler-Lagrange Equations of Motion

Snake robots are categorized in the class of *simple* mechanical systems, where the Lagrangian $L(q, \dot{q})$ is defined as the difference between the kinetic energy $K(q, \dot{q})$ and the potential energy $P(q)$ of the system [Bullo (2005)]. Since the planar snake robot is not subject to any potential field, i.e. $-\nabla P(q) = 0$, we may write the Lagrangian equal to the kinetic energy, which is the sum of the translational and rotational kinetic energy of the robot

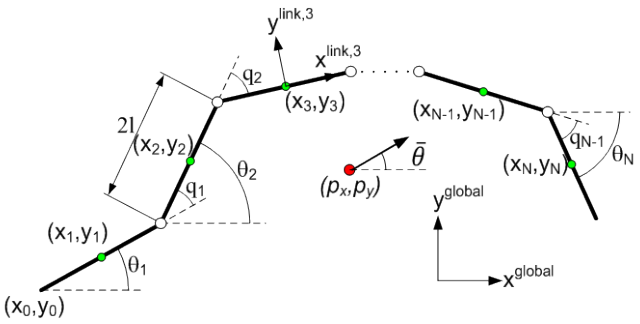

Fig. 1. Kinematic parameters of the snake robot

$$L(q, \dot{q}) = K(q, \dot{q}) = \frac{1}{2}m\sum_{i=1}^{N}(\dot{x}_i^2 + \dot{y}_i^2) + \frac{1}{2}J\sum_{i=1}^{N}\dot{\theta}_i^2 \tag{8}$$

where m and J denote the mass and moment of inertia of a link, respectively. Using the definition of the Lagrangian from (8), one can write the equations of motion of a snake robot without sideslip constraints as

$$\frac{d}{dt}\left(\frac{\partial L(q,\dot{q})}{\partial \dot{q}_i}\right) - \frac{\partial L(q,\dot{q})}{\partial q_i} = \left(B(q)\tau - \tau_f\right)_i$$

where $i \in \{1, \dots, N+2\}$, $B(q) = \left[e_j\right] \in \mathbb{R}^{(N+2)\times(N-1)}$ is the actuator configuration matrix where e_j denotes the j-th standard basis vector in $\mathbb{R}^{N-1}$. Furthermore, $B(q)\tau \in \mathbb{R}^{N+2}$ where $\tau = [\tau_1, \dots, \tau_{N-1}]^T \in \mathbb{R}^{N-1}$ stands for the generalized forces resulting from the control inputs, and $\tau_f = \left[\tau_{f_1}, \dots, \tau_{f_{N+2}}\right]^T \in \mathbb{R}^{N+2}$ denotes the viscous and Coulomb ground friction forces acting on $(N+2)$-DOF of the system. The equations of motion can also be written as a second order differential equation in the form

$$M(q)\ddot{q} + C(q,\dot{q})\dot{q} = B(q)\tau - \tau_f \tag{9}$$

where $M(q) \in \mathbb{R}^{(N+2)\times(N+2)}$ is the symmetric positive definite matrix of inertia, $C(q,\dot{q}) \in \mathbb{R}^{(N+2)\times(N+2)}$ denotes the matrix of Coriolis and centrifugal forces, and the right-hand side (RHS) terms denote the external forces acting on the system. Since $\text{rank}[B(q)] < \dim(q)$ the system is underactuated. This underactuation represents lack of direct control on the heading and position of the CM of the robot w.r.t. the inertial frame.

1.3 The Ground Friction Model

In this subsection, both viscous and Coulomb friction models are used for capturing the essential properties of the *anisotropic* ground friction. For modeling the friction, we first define the rotation matrix for mapping from the global frame to the local frame of link i as

$$R_i^{\text{global}} = \begin{bmatrix} \cos\theta_i & -\sin\theta_i \\ \sin\theta_i & \cos\theta_i \end{bmatrix} \tag{10}$$

The total friction acting on link i is defined as the sum of the viscous and Coulomb friction forces for that link, which are denoted by f_{v_i} and f_{c_i}, respectively, and which gives

$$f_i^{\text{link}} = f_{c_i} + f_{v_i} \tag{11}$$

Assuming equal friction coefficients for all the links, we write the model of the friction for each individual link i as

$$f_{c_i} = mg\left(\mu_t \text{sgn}\left(v_t^{\text{link},i}\right) + \mu_n \,\text{sgn}\left(v_n^{\text{link},i}\right)\right) \tag{12}$$

$$f_{v_i} = \left(c_t v_t^{\text{link},i} + c_n v_n^{\text{link},i}\right) \tag{13}$$

where $i \in \{1, \dots, N\}$, g is the gravitational acceleration, and μ_t and μ_n denote Coulomb friction coefficients in the tangential and normal direction of the motion of the link, respectively. Furthermore, c_t and c_n denote viscous friction coefficients in the tangential and normal direction, respectively, and $v_n^{\text{link},i}$ and $v_t^{\text{link},i}$ denote the linear velocity of the i-th link in the normal and tangential direction, respectively. Using (4) and (10), the velocities of the links in the local frame link can be written in terms of the velocities of the links in the global frame

$$v_i^{\text{link}} = \begin{bmatrix} v_t^{\text{link},i} \\ v_n^{\text{link},i} \end{bmatrix} = \left(R_i^{\text{global}}\right)^T \begin{bmatrix} \dot{x}_i \\ \dot{y}_i \end{bmatrix} \tag{14}$$

Finally, we map the friction force acting on each link to the global frame using

$$f_{\text{link},i}^{\text{global}} = R_i^{\text{global}} f_i^{\text{link}} \tag{15}$$

and we may write τ_f in (9) as

$$\tau_f = \textstyle\sum_{i=1}^{N} \mathcal{J}_i^T f_{\text{link},i}^{\text{global}} \tag{16}$$

where $\mathcal{J}_i^T$ denotes the transpose of the *Jacobian* matrix of the CM of the i-th link.

Remark 1. *As argued in Liljebäck* et al. *(2012), the motion of a snake robot with anisotropic viscous ground friction is qualitatively (but not quantitatively) similar as with anisotropic Coulomb friction. However, a viscous friction model is less complex w.r.t. control design and analysis. Accordingly, we employ a viscous ground friction model in this paper.*

1.4 Partial Feedback Linearization

A common method for nonlinear control of mechanical systems is full-state feedback linearization. This approach is not applicable to underactuated mechanical systems, which have fewer inputs than DOF. However, it is still possible to linearize the dynamic equations which correspond to the actuated DOF, which is called *collocated partial feedback linearization* [see e.g. Spong (1994)]. A similar technique is considered in Liljebäck *et al.* (2012), but for the sake of completeness, we present the approach here. To this end, we separate the dynamical equations of the robot given by (9) into two subsets by taking

$$q = [q_a, q_u]^T \in \mathbb{R}^{N+2}$$

where $q_a = [q_1, \dots, q_{N-1}]^T \in \mathbb{R}^{N-1}$ denotes the actuated shape variables, and $q_u = \left[\bar{\theta}, p_x, p_y\right]^T \in \mathbb{R}^3$ denotes the unactuated position variables, as

$$m_{11}(q_a)\ddot{q}_a + m_{12}(q_a)\ddot{q}_u + h_1(q, \dot{q}) = \psi \in \mathbb{R}^{N-1} \tag{17}$$

$$m_{21}(q_a)\ddot{q}_a + m_{22}(q_a)\ddot{q}_u + h_2(q, \dot{q}) = 0_{3\times 1} \in \mathbb{R}^3 \tag{18}$$

in which $h_{1,2}(q, \dot{q})$ include all the contributions of the Coriolis, centrifugal and friction forces, and $\psi \in \mathbb{R}^{N-1}$ denotes the non-zero part of the vector of control forces $B(q)\tau = [\psi, 0_{3\times 1}]^T \in \mathbb{R}^3$. From (18) we have

$$\ddot{q}_u = -m_{22}^{-1}(h_2 + m_{21}\ddot{q}_a) \in \mathbb{R}^3 \tag{19}$$

Substituting (19) into (17) yields

$$(m_{11} - m_{12}m_{22}^{-1}m_{21})\ddot{q}_a - (m_{12}m_{22}^{-1})h_2 + h_1 = \psi \tag{20}$$

If we apply the global change of the vector of control inputs

$$\psi = (m_{11} - m_{12}m_{22}^{-1}m_{21})\vartheta - (m_{12}m_{22}^{-1})h_2 + h_1 \tag{21}$$

where $\vartheta = [\vartheta_1, \vartheta_2, \dots, \vartheta_{N-1}]^T \in \mathbb{R}^{N-1}$ is the vector of new control inputs, then the system (17)-(18) can be written in partially feedback linearized form as

$$\ddot{q}_a = \vartheta \in \mathbb{R}^{N-1} \tag{22a}$$

$$\ddot{q}_u = \mathcal{D}(q, \dot{q}) + \mathcal{C}(q_a)\vartheta \in \mathbb{R}^3 \tag{22b}$$

with

$$\mathcal{D}(q, \dot{q}) = -m_{22}^{-1}(q_a)h_2(q, \dot{q}) = [f_N, f_{N+1}, f_{N+2}]^T \in \mathbb{R}^3$$

$$\mathcal{C}(q_a) = -m_{22}^{-1}(q_a)m_{21}(q_a) = [\beta_i(q_a), 0, 0]^T \in \mathbb{R}^{3\times(N-1)}$$

where $\beta_i \in \mathbb{R}$ is a smooth function, and f_N, f_{N+1} and f_{N+2} include the friction forces acting on the passive DOF. The dynamic model given by (22) is in the form of a *control-affine* system. In particular, the *drift vector field*

$$f(q, \dot{q}) = \left[\dot{q}_a, \dot{q}_u, 0_{(N-1)\times 1}, \mathcal{D}(q, \dot{q})\right]^T \in \mathbb{R}^{2N+4}$$

represents the dynamical behavior of the system when the input is zero. Furthermore, the *control vector fields* as the columns of the matrix given by

$$g(q_a) = \begin{bmatrix} 0_{(N+2)\times(N-1)} \\ I_{N-1} \\ [\beta_1(q_a), \dots, \beta_{N-1}(q_a)] \\ 0_{2\times(N-1)} \end{bmatrix} \in \mathbb{R}^{(2N+4)\times(N-1)}$$

enable us to control the internal shape and consequently the heading and position of the snake robot. We can write (22) in a more detail form as

$$\ddot{q}_a = \vartheta \in \mathbb{R}^{N-1} \tag{23a}$$

$$\ddot{\bar{\theta}} = f_N(q, \dot{q}) + \beta_i(q_a)\vartheta^i \in \mathbb{R} \tag{23b}$$

$$\ddot{p}_x = f_{N+1}(q, \dot{q}) \in \mathbb{R} \tag{23c}$$

$$\ddot{p}_y = f_{N+2}(q, \dot{q}) \in \mathbb{R} \tag{23d}$$

Note that the summation convention is applied to (23b), where $i \in \{1, \dots, N-1\}$, and also note that the friction forces in (23a) are compensated by the control action in (21).

3. CONTROLLABILITY ANALYSIS

In this section, we analyze the possibility of controlling the heading of the snake robot in the absence of $f_N(q, \dot{q})$, which is the term that includes all the contributions of the Coriolis, centrifugal, and external dissipative forces acting on the angular dynamics of the system. In particular, we are interested to perform this analysis because our underactuated control design is based on the cancellation of this term. Since our control design is a guidance-based path following approach,

i.e. defining a desired heading angle through a guidance law and designing a controller to track this angle, here we only consider the controllability properties of the angular subsystem of the equations of motions, which is given by (23a)-(23b). According to the partially feedback linearized model (23), one can derive the control and the drift vector fields of (23a)-(23b) when $f_N(q,\dot{q}) \equiv 0$, as

$$f = \sum_{i=1}^{N-1} \dot{q}_i \frac{\partial}{\partial q_i} + \dot{\bar{\theta}} \frac{\partial}{\partial \bar{\theta}}$$

$$g_i = \frac{\partial}{\partial \dot{q}_i} + \beta_i(q_a) \frac{\partial}{\partial \dot{\bar{\theta}}}$$

with $i \in \{1, \dots, N-1\}$. Due to space restrictions, we do not show the complete calculations here. We present the results of an *accessibility* analysis based on the *accessibility rank condition,* see e.g. Bullo (2005), in the following Theorem.

Theorem I. *In the absence of the drift term $f_N(q,\dot{q})$, the subsystem (23a)-(23b) is strongly accessible.*

Proof: for analyzing the accessibility of the subsystem (23a)-(23b) in the absence of the term $f_N(q,\dot{q})$, which is the necessary condition for controllability, based on accessibility rank condition we must find $2N$ linearly independent vector fields that span $2N$-dimensional state space of the subsystem (23a)-(23b). These vector fields are given by

$$g_i, [f, g_i], \left[g_{i_0}, [f, g_{j_0}]\right], \left[f, \left[g_{i_0}, [f, g_{j_0}]\right]\right]$$

with $i, i_0, j_0 \in \{1, \dots, N-1\}$. This implies that in the absence of $f_N(q,\dot{q})$, the system is strongly accessible. ■

However, for the above case, the *Sussmann sufficient condition for small time local controllability (STLC)*, see e.g. Bullo (2005), does not hold since the *bad brackets* of the form

$$\left[g_j, [f, g_i]\right]$$

cannot be written as linear combination of lower order *good brackets*, and the STLC property of the system could not be concluded in this case.

4. CONTROL DESIGN OBJECTIVES

In this section, we state our control design objectives which will be followed throughout the paper. In particular, we divide these objectives into three parts which in general correspond to the control of the internal shape variables, i.e. $q_a = [q_1, \dots, q_{N-1}]^T \in \mathbb{R}^{N-1}$, the heading angle $\bar{\theta}$, and the position of the CM of the robot (p_x, p_y). To this end, we define an output vector for the dynamical system (23) as

$$Y = \left[\tilde{q}_1, \dots, \tilde{q}_{N-1}, \tilde{\theta}, \tilde{p}_x, \tilde{p}_y\right]^T \in \mathbb{R}^{N+2} \tag{24}$$

in which every element denotes the error of the corresponding generalized coordinate w.r.t. a reference signal which will be defined in the next sections. In particular, for the internal shape variables we define the control objective as

$$\lim_{t\to+\infty} \|\tilde{q}_i\| = 0 \tag{25}$$

where $i \in \{1, \dots, N-1\}$. For the orientation of the robot in the plane, we define the control objective for the solutions of the heading error dynamics to exponentially converge to an arbitrary small neighborhood of the origin such that

$$\lim_{t\to+\infty} \|\tilde{\theta}\| \leq \epsilon_H \tag{26}$$

where $\epsilon_H \in \mathbb{R}^+$ is a small constant. Finally, for the position of the CM of the robot which has inherent oscillatory behavior while the robot is performing the gait pattern lateral undulation, we define the control objective as converging to and following a desired planar path such that

$$\lim_{t\to+\infty} \|\tilde{p}_{x,y}\| \leq \epsilon_{CM} \tag{27}$$

where $\epsilon_{CM} \in \mathbb{R}^+$ is a small constant. This implies that the position of the CM oscillates around the desired path.

5. THE JOINT CONTROL LAW

It is known that the locomotion of an N-link snake robot in accordance with the serpenoid curve, i.e. lateral undulation, is achieved if the joints of the robot move according to the reference joint trajectory given by [Hirose (1993)]

$$q_{\mathrm{ref,i}} = \alpha \sin(\omega t + (i-1)\delta) + \phi_0 \tag{28}$$

where $i \in \{1, \dots, N-1\}$, α denotes the amplitude of the sinusoidal joint motion, ω denotes the angular frequency, δ is a phase shift that is used to keep the joints *out of phase*, and ϕ_0 is a joint offset that is identical for all of the joints. In particular, we use ϕ_0 as a ***virtual control input*** for our underactuated control design in Section 6.

We choose an exponentially stabilizing control law for the joints of the snake robot in the form

$$\vartheta_i = \ddot{q}_{\mathrm{ref},i} + k_d(\dot{q}_{\mathrm{ref},i} - \dot{q}_i) + k_p(q_{\mathrm{ref},i} - q_i) \tag{29}$$

where $\vartheta_i \in \{\vartheta_1, \dots, \vartheta_{N-1}\}$ denotes the input to the i-th joint, while $k_p > 0$ and $k_d > 0$ are controller gains which are taken to be equal for all the links since they have similar inertial parameters. We define the position and velocity tracking errors for the i-th joint, respectively, as

$$\tilde{q}_i = q_{\mathrm{ref,i}} - q_i, \;\; \dot{\tilde{q}}_i = \dot{q}_{\mathrm{ref},i} - \dot{q}_i$$

By substituting (29) into (23a), the equation of the error dynamics for the joints of the snake robot can be given as

$$\ddot{\tilde{q}}_i + k_d \dot{\tilde{q}}_i + k_p \tilde{q}_i = 0 \tag{30}$$

which clearly has a globally exponentially stable equilibrium at the origin. This implies that the joint tracking errors converge to zero exponentially, regardless of the initial conditions.

6. UNDERACTUATED CONTROL

In this section, we analytically show that it is possible to use ϕ_0 in the reference joint trajectory as a virtual control input, to make the heading angle of the snake robot track a desired heading angle. With the reference joint trajectory (28), the desired trajectories for the joints of the snake robot are composed of a sinusoidal part and an offset. In particular, by taking $S_i = \alpha \sin(\omega t + (i-1)\delta)$, the reference trajectory of the i-th joint can be rewritten in the form

$$q_{\mathrm{ref},i} = S_i + \phi_0$$

It was illustrated in Liljebäck *et al.* (2012) how the offset value ϕ_0 affects the orientation of the snake robot in the plane. Building further on this insight, we consider the offset value ϕ_0 as a virtual control input for the heading dynamics of the robot. Furthermore, we design this term to make the

heading dynamics exponentially converge to the desired heading angle. In particular, we use this virtual input for shaping the dynamics of the heading which by inserting (29) into (23b), can be written in the closed-loop form as

$$\ddot{\bar{\theta}} = f_N + \sum_{i=1}^{N-1} \beta_i \vartheta_i = f_N + \sum_{i=1}^{N-1} \beta_i \left(\ddot{S}_i + k_d \dot{S}_i + k_p S_i - k_p q_i - k_d \dot{q}_i\right) + \sum_{i=1}^{N-1} \beta_i k_p \phi_0 + \sum_{i=1}^{N-1} \beta_i \left(\ddot{\phi}_0 + k_d \dot{\phi}_0\right) \quad (31)$$

We take the virtual control input in the form

$$\phi_0 = \frac{1}{\sum_{i=1}^{N-1} \beta_i k_p} \left(-f_N - \sum_{i=1}^{N-1} \beta_i \left(\ddot{S}_i + k_d \dot{S}_i + k_p S_i - k_p q_i - k_d \dot{q}_i\right) + \sigma\right) \quad (32)$$

where σ is a new control input. Note that since the matrix of inertia is a positive-definite matrix-valued function of configurations [Lewis (2007)], β_i is negative-definite for all $i \in \{1, \dots, N-1\}$, which implies that (32) is well-defined. With the above choice of ϕ_0, the heading dynamics (31) takes the form

$$\ddot{\bar{\theta}} = \sigma + \sum_{i=1}^{N-1} \beta_i \left(\ddot{\phi}_0 + k_d \dot{\phi}_0\right) \quad (33)$$

We define the error variable for the heading angle as

$$\tilde{\theta} = \theta_d - \bar{\theta}$$

where θ_d denotes the desired heading angle of the snake robot. We take the new control input in (32) as

$$\sigma = k_{\bar{\theta},P} \tilde{\theta} + k_{\bar{\theta},D} \dot{\tilde{\theta}} + \ddot{\theta}_d \quad (34)$$

By inserting (34) into (33), we can write the error dynamics for the heading angle of the snake robot as

$$\ddot{\tilde{\theta}} + k_{\bar{\theta},D} \dot{\tilde{\theta}} + k_{\bar{\theta},P} \tilde{\theta} = -\sum_{i=1}^{N-1} \beta_i \left(\ddot{\phi}_0 + k_d \dot{\phi}_0\right) \quad (35)$$

For the sake of clarity, let us denote the RHS term of (35) as

$$\Phi = -\sum_{i=1}^{N-1} \beta_i \left(\ddot{\phi}_0 + k_d \dot{\phi}_0\right) \quad (36)$$

The time-derivatives $\dot{\phi}_0$ and $\ddot{\phi}_0$ are complex functions of time which cannot easily be expressed analytically. However, we can obtain approximate analytical expressions for these time-derivatives by filtering the signal ϕ_0, e.g. by using a low-pass filtering reference model, see e.g. Liljebäck *et al.* (2012), as

$$\frac{d}{dt} \begin{bmatrix} \phi_{0_f} \\ \dot{\phi}_{0_f} \end{bmatrix} = \begin{bmatrix} 0 & 1 \\ -\omega_n^2 & -2\zeta\omega_n \end{bmatrix} \begin{bmatrix} \phi_{0_f} \\ \dot{\phi}_{0_f} \end{bmatrix} + \begin{bmatrix} 0 \\ \omega_n^2 \end{bmatrix} \phi_0 \quad (37)$$

with the natural frequency ω_n and the damping ratio ζ. The input to this filter is ϕ_0, and we can find approximations of $\dot{\phi}_0$ and $\ddot{\phi}_0$, which we denote by $\dot{\phi}_{0_f}$ and $\ddot{\phi}_{0_f}$, respectively. Subsequently, we can approximate (36) as

$$\Phi \cong \Phi_f = -\sum_{i=1}^{N-1} \beta_i \left(\ddot{\phi}_{0_f} + k_d \dot{\phi}_{0_f}\right) \quad (38)$$

We consider (38) as a time-varying perturbation term, and we aim to analyze the stability of the heading error dynamics in the presence of this perturbation. In the case where the RHS term of (35) is identically zero, i.e. $\Phi \equiv 0$, the equation of the heading error dynamics (35) has clearly an exponentially stable equilibrium at the origin whenever $k_{\bar{\theta},D} > 0$ and $k_{\bar{\theta},P} > 0$. However, this will generally not be the case. We therefore consider the RHS term as a *non-vanishing perturbation* term that is perturbing the exponentially stable nominal LHS part.

Before proceeding to the perturbation analysis, we need to analyze the angular subsystem (23a)-(23b) in the closed-loop form. In particular, by inserting (32) along with the filtered signal (38) into (31), we obtain the dynamical equations corresponding to angular dynamics (23a)-(23b) in the form

$$\ddot{q}_a = \vartheta \in \mathbb{R}^{N-1} \quad (39a)$$

$$\ddot{\bar{\theta}} = \ddot{\theta}_d + k_{\bar{\theta},D} \dot{\tilde{\theta}} + k_{\bar{\theta},P} \tilde{\theta} + \Phi_f \in \mathbb{R} \quad (39b)$$

However, in the current form, this subsystem is not controllable. This problem along with the solution is shown in the following remark.

Remark 2. *By taking* $l_1\left(\bar{\theta}, \dot{\bar{\theta}}, t\right) = \ddot{\theta}_d + k_{\bar{\theta},D} \dot{\tilde{\theta}} + k_{\bar{\theta},P} \tilde{\theta} + \Phi_f$*, the control and the drift vector fields of (39) can be, respectively, given by*

$$g_i = \frac{\partial}{\partial \dot{q}_i}$$

$$f = \sum_{i=1}^{N-1} \dot{q}_i \frac{\partial}{\partial q_i} + \dot{\bar{\theta}} \frac{\partial}{\partial \bar{\theta}} + l_1\left(\bar{\theta}, \dot{\bar{\theta}}, t\right) \frac{\partial}{\partial \dot{\bar{\theta}}}$$

One can verify that the only non-zero brackets of the system are

$$g_i, [f, g_i]$$

with $i \in \{1, \dots, N-1\}$*, and all other brackets of the system (either of the type* good *or* bad*, see e.g. Bullo (2005)) evaluate to zero. This implies that the system is not accessible (and consequently uncontrollable) in this from. To solve this problem, we can redefine* ϕ_0 *as*

$$\phi_{0_{\text{new}}} = \frac{\phi_0}{1+\varepsilon} - \frac{1}{\sum_{i=1}^{N-1} \beta_i k_p} \frac{\varepsilon}{1+\varepsilon} (f_N + \sigma) \quad (40)$$

where $0 < \varepsilon \ll 1$*. This will lead to an* exact cancellation *of the term* f_N*, but* un-exact cancellation *of the control vector fields in (39b). Thus, we have the system in the form*

$$\ddot{q}_a = \vartheta \quad (41a)$$

$$\ddot{\bar{\theta}} = \ddot{\theta}_d + k_{\bar{\theta},D} \dot{\tilde{\theta}} + k_{\bar{\theta},P} \tilde{\theta} + \mathcal{L}(q_a, \dot{q}_a, t) \quad (41b)$$

where $\mathcal{L}(\cdot)$ *denotes the remaining terms from un-exact cancellation of the control vector fields that is represented by a smooth function in the form*

$$\mathcal{L}(\cdot) = \frac{\varepsilon}{1+\varepsilon} \left(\sum_{i=1}^{N-1} \beta_i \left(\ddot{S}_i + k_d \dot{S}_i + k_p S_i - k_p q_i - k_d \dot{q}_i\right)\right) + \Phi_f \quad (42)$$

This function is bounded as long as the dynamics of the system is stable with (29). We denote this bound by

$$\|\mathcal{L}(\cdot)\| \leq \Gamma \quad (43)$$

where $\Gamma \in \mathbb{R}^+$ *is a constant. In this form, the control and the drift vector fields of (41) can be given by*

$$g_i = \frac{\partial}{\partial \dot{q}_i} + \frac{\varepsilon}{1+\varepsilon} \beta_i \frac{\partial}{\partial \dot{\bar{\theta}}}$$

$$f = \sum_{i=1}^{N-1} \dot{q}_i \frac{\partial}{\partial q_i} + \dot{\bar{\theta}} \frac{\partial}{\partial \bar{\theta}} + l_1(q, \dot{q}, t) \frac{\partial}{\partial \dot{\bar{\theta}}}$$

The linearly independent vector fields given by

$$g_i, [f, g_i], \left[g_{i_0}, [f, g_{j_0}]\right], \left[f, \left[g_{i_0}, [f, g_{j_0}]\right]\right]$$

with $i, i_0, j_0 \in \{1, \dots, N-1\}$*, span the* $2N$*-dimensional state space of (41), and the system is strongly accessible. Furthermore, (41b) has an exponentially stable part which is perturbed by a bounded non-vanishing perturbation. In addition, in this perturbed form, we cannot study the origin as an equilibrium point; however, based on the perturbation analysis given in Khalil (2002), Chapter 9, we can still expect the trajectories of (41b) to exponentially converge to an open ball in neighborhood of the origin.*

We can write the state space model of the heading dynamics (41b) as

$$\frac{d}{dt}\begin{bmatrix}\tilde{\theta}\\ \dot{\tilde{\theta}}\end{bmatrix} = \begin{bmatrix}0 & 1\\ -k_{\bar{\theta},P} & -k_{\bar{\theta},D}\end{bmatrix}\begin{bmatrix}\tilde{\theta}\\ \dot{\tilde{\theta}}\end{bmatrix} + \begin{bmatrix}0\\ \mathcal{L}\end{bmatrix} \tag{44}$$

where the function $\mathcal{L}(\cdot)$ is defined in (42). Now the question is "what can we say about the stability of this perturbed system?". We answer this question through the following perturbation analysis.

Remark 3. *Following the perturbation analysis given in Khalil (2002), our mathematical proof strategy for ultimate boundedness of the trajectories of the perturbed system (44) is in the way that we first find a Lyapunov function for the exponentially stable nominal part of (44), and we show that the time-derivative of this Lyapunov function along the trajectories of the perturbed system is negative definite inside a specific boundary. Then we define two open sets* Ω_1 *and* Ω_2 *inside this boundary such that one of these sets is an open subset of the other set (*$\Omega_1 \subset \Omega_2$*). The negative definiteness of the time-derivative of the Lyapunov function inside the boundary of these sets implies the positive invariancy of these sets. Accordingly, the trajectories of the perturbed system (44), which start in this boundary, decrease exponentially until they reach the positive invariant subset* Ω_1 *in a finite time. Furthermore, the positive invariancy implies that the trajectories cannot leave this set for all future time. This enables us to find an ultimate bound for the trajectories of the perturbed system.*

Note that according to the *Converse Theorem* [Khalil (2002)], the exponentially stability of the origin of the nominal part of (44), which is given by the linear map

$$A = \begin{bmatrix}0 & 1\\ -k_{\bar{\theta},P} & -k_{\bar{\theta},D}\end{bmatrix}$$

ensures that for the Lyapunov equation

$$PA + A^T P = -I$$

with any given symmetric positive definite matrix I, there exists a symmetric positive definite matrix P as the solution, which we denote by

$$P = \begin{bmatrix}p_1 & p_2\\ p_2 & p_4\end{bmatrix}$$

If we denote the state vector of (44) by $\tilde{\theta}_s = \left[\tilde{\theta}, \dot{\tilde{\theta}}\right]^T \in \mathbb{R}^2$, and the exponentially stable nominal part of (44) with $F(\tilde{\theta}_s) = A\tilde{\theta}_s$, the linear part of (44) has a quadratic Lyapunov function in the form $V(\tilde{\theta}_s) = \tilde{\theta}_s^T P \tilde{\theta}_s$. Moreover, this Lyapunov function satisfies the following inequalities [Khalil (2002)]

$$\lambda_{\min}\|\tilde{\theta}_s\|^2 \le V(\tilde{\theta}_s) \le \lambda_{\max}\|\tilde{\theta}_s\|^2 \tag{45a}$$

$$\frac{\partial V(\tilde{\theta}_s)}{\partial \tilde{\theta}_s} F(\tilde{\theta}_s) \le -c_3\|\tilde{\theta}_s\|^2 \tag{45b}$$

$$\left\|\frac{\partial V(\tilde{\theta}_s)}{\partial \tilde{\theta}_s}\right\| \le c_4\|\tilde{\theta}_s\| \tag{45c}$$

where $c_{3,4}$ are positive constants, and $\lambda_{\min}$ and $\lambda_{\max}$ denote the minimum and maximum eigenvalues of matrix A, respectively. Accordingly, the Lyapunov function for the linear part of (44) has the form

$$V(\tilde{\theta}_s) = p_1\tilde{\theta}^2 + p_4\dot{\tilde{\theta}}^2 + 2p_1\tilde{\theta}\dot{\tilde{\theta}} \tag{46}$$

We take (46) as a Lyapunov function candidate for the perturbed system. The derivative of (46) along the trajectories of the perturbed system (44) can be written as

$$\dot{V}(\tilde{\theta}_s) = -2k_{\bar{\theta},P}\tilde{\theta}^2 + (2p_2 - 2p_4k_{\bar{\theta},P})\dot{\tilde{\theta}}^2 + (2p_1 - 2p_2k_{\bar{\theta},D} - 2p_4k_{\bar{\theta},P})\tilde{\theta}\dot{\tilde{\theta}} + \left(2p_4\dot{\tilde{\theta}} + 2p_2\tilde{\theta}\right)\mathcal{L} \tag{47}$$

The first three RHS terms of (47) denote the derivative of (46) along the trajectories of the nominal system, i.e. linear part of (44), which we denote by $\dot{V}_{\text{nom}}(\tilde{\theta}_s)$. Furthermore, the last term stands for the derivative of (46) along the perturbation term, which we denote by $\dot{V}_{\text{pert}}(\tilde{\theta}_s)$. Subsequently, we can write (47) as

$$\dot{V}(\tilde{\theta}_s) = \dot{V}_{\text{nom}}(\tilde{\theta}_s) + \dot{V}_{\text{pert}}(\tilde{\theta}_s) \tag{48}$$

Applying the boundary given by (45b) to $\dot{V}_{\text{nom}}(\tilde{\theta}_s)$ we obtain

$$\dot{V}_{\text{nom}}(\tilde{\theta}_s) \le -c_3\|\tilde{\theta}_s\|^2 \tag{49}$$

By considering the assumption of the boundedness of the perturbing term $\|\mathcal{L}\| \le \Gamma$ along with (45c), we can write

$$\dot{V}_{\text{pert}}(\tilde{\theta}_s) = \left(2p_4\dot{\tilde{\theta}} + 2p_2\tilde{\theta}\right)\mathcal{L} \le c_4\|\tilde{\theta}_s\|\Gamma \tag{50}$$

From (49)-(50) we have

$$\dot{V}(\tilde{\theta}_s) \le -c_3\|\tilde{\theta}_s\|^2 + c_4\|\tilde{\theta}_s\|\Gamma \tag{51}$$

By introducing a constant $0 < \kappa < 1$ we have

$$\dot{V}(\tilde{\theta}_s) \le -(1-\kappa)c_3\|\tilde{\theta}_s\|^2 - \kappa c_3\|\tilde{\theta}_s\|^2 + c_4\|\tilde{\theta}_s\|\Gamma \le -(1-\kappa)c_3\|\tilde{\theta}_s\|^2, \quad \forall\, \mu = \frac{\Gamma c_4}{\kappa c_3} \le \|\tilde{\theta}_s\| \le r \tag{52}$$

where r is a positive constant. If we choose r sufficiently larger than μ, then we can find a non-empty set $\Lambda = \{\varepsilon_1 \le V(\tilde{\theta}_s) \le \varepsilon_2\}$, such that Λ is contained in $\{\mu \le \|\tilde{\theta}_s\| \le r\}$. Since $\dot{V}(\tilde{\theta}_s)$ is negative on the boundaries Ω_1 and Ω_2, the sets $\Omega_1 = \{V(\tilde{\theta}_s) \le \varepsilon_1\}$ and $\Omega_2 = \{V(\tilde{\theta}_s) \le \varepsilon_2\}$ are positively invariant. Furthermore, all the trajectories starting in Λ, will move in the direction where $\dot{V}(\tilde{\theta}_s)$ decreases. In other words, inside Λ the solutions of (44) satisfy (52) and behave as the origin is exponentially stable that is [Khalil (2002)]

$$\|\tilde{\theta}_s\| < k\|\tilde{\theta}_s(0)\|\exp(-\lambda t), \quad \forall\, 0 < t < T \tag{53}$$

with positive constants k and λ. According to (53), the trajectories that start in Ω_2 decrease exponentially until they reach to the positive invariant set Ω_1 and stay there for all future time. In (53), T denotes the finite time interval that the trajectories enter from Ω_1 to Ω_2. According to the condition $\mu = \frac{\Gamma c_4}{\kappa c_3} \leq \|\tilde{\theta}_s\| \leq r$ for $\dot{V}(\tilde{\theta}_s)$ to be negative definite, we should chose ε_1 and ε_2 to ensure that $\Omega_1 \subset B_\mu$ and $\Omega_2 \subset B_r$, where B_μ and B_r denote the open balls of radius μ and r, respectively, centered at the origin of the state-manifold of (44). To this end, from (45a) we have

$$\lambda_{\min}\|\tilde{\theta}_s\|^2 \leq V(\tilde{\theta}_s) \leq \lambda_{\max}\|\tilde{\theta}_s\|^2 \qquad (54)$$

From left inequality we obtain $\lambda_{\min}\|\tilde{\theta}_s\|^2 \leq V(\tilde{\theta}_s) \leq \varepsilon_2$ which implies $\|\tilde{\theta}_s\| \leq \sqrt{\varepsilon_2/\lambda_{\min}}$. Taking $\varepsilon_2 = \lambda_{\min} r^2$ implies $\Omega_2 \subset B_r$. From the right inequality we have $\varepsilon_1 \leq V(\tilde{\theta}_s) \leq \lambda_{\max}\|\tilde{\theta}_s\|^2$ which implies $\|\tilde{\theta}_s\| \geq \sqrt{\varepsilon_1/\lambda_{\max}}$. Taking $\varepsilon_1 = \lambda_{\max}\mu^2$ implies $B_\mu \subset \Omega_1$.

To complete our analysis we need to find the ultimate bound on trajectories $\|\tilde{\theta}_s\|$ after finite time T that they enter to Ω_1. To this end and following Khalil (2002), we use the fact that when the trajectories enter the set Ω_1 then we have

$$V(\tilde{\theta}_s) \leq \varepsilon_1$$

this implies

$$\lambda_{\min}\|\tilde{\theta}_s\|^2 \leq \varepsilon_1$$

which gives

$$\|\tilde{\theta}_s\| \leq \sqrt{\varepsilon_1/\lambda_{\min}}$$

Applying the requirement of the foregoing arguments on ε_1 that was given by $\varepsilon_1 = \lambda_{\max}\mu^2$ we obtain

$$\|\tilde{\theta}_s\| \leq \mu\sqrt{\lambda_{\max}/\lambda_{\min}}$$

By considering the definition of μ in (52) as $\mu = \frac{\Gamma c_4}{\kappa c_3}$, we obtain the ultimate bound on $\|\tilde{\theta}_s\|$ as

$$\|\tilde{\theta}_s\| \leq \frac{\Gamma c_4}{\kappa c_3}\sqrt{\lambda_{\max}/\lambda_{\min}} \qquad (55)$$

The trajectories of the perturbed system are restricted to this bound after the finite time *T*. we collect the foregoing arguments in the following theorem.

Theorem II. *Assuming the boundedness of the perturbation term (42), if the trajectories of the perturbed system (44) start in a set where the derivative of the Lyapunov function (46) that satisfies (45) along the trajectories of (44) is negative definite, then these trajectories decrease exponentially until they reach a positive invariant bounded open subset of the state-manifold of (44) in a finite time T, and the trajectories of (44) are bounded by the ultimate bound (55) for all future time.*

7. THE PATH FOLLOWING GUIDANCE LAW

In this section, we introduce a guidance law that is used for defining the desired heading angle of the snake robot for following a planar path. We use a guidance law such that the position of the CM of the snake robot denoted by (p_x, p_y) follows a desired path which in (x, y) plane is defined by the pair

$$p_d(\gamma) = \big(p_{xd}(\gamma), p_{yd}(\gamma)\big) \qquad (56)$$

where γ denotes the path parameterization variable. The guidance law that we use is in the form

$$\theta_d = \text{atan2}(\tilde{p}_y, \tilde{p}_x) \qquad (57)$$

in which

$$\tilde{p}_x = p_{xd}(\gamma) - p_x, \;\; \tilde{p}_y = p_{yd}(\gamma) - p_y \qquad (58)$$

denote the error of the (p_x, p_y) w.r.t. the desired path coordinates (p_{xd}, p_{yd}), respectively. Fig. 2 is a geometric presentation of the idea of our guidance-based control design. Finally, we conjecture that with the proposed guidance-based path following control strategy, the position of the CM of the robot converges to the desired planar path. As a support of this conjecture, we provide in Section 8 simulation results which show that the snake robot successfully converges to the desired path.

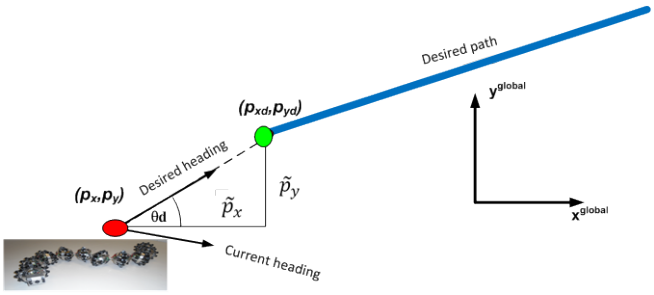

Fig. 2. The red dot shows the initial position of the CM of the snake robot and $(\tilde{p}_x, \tilde{p}_y)$ shows the initial error. Guidance-based control strategy steers the red dot towards the desired path depicted as blue line, by making the current heading angle equal to the desired heading angle at each moment. The coordinates of the desired point on the path (shown by the green point) gradually change in accordance with the path parameterization variable γ.

8. SIMULATION RESULTS

In this section, the results of the simulation of the path following controller for a snake robot are presented. We simulate our control approach on a 4-link snake robot. However, these results are generalizable to snake robots with more links. The inertial parameters of the links were $m = 0.1$ kg, $l = 0.14$ m, and $J = 0.0016$ kgm^2. The viscous friction coefficients were $c_n = 20$ and $c_t = 1$. The parameters of the reference joint trajectories were $\alpha = \frac{\pi}{6}$ rad, $\omega = \frac{2\pi}{5}$ rad/s, and $\delta = \frac{2\pi}{9}$ rad. The joint controller gains in (29) were tuned as $k_p = 500$ and $k_d = 200$. Finally, the gains in (34) were chosen as $k_{\bar{\theta},P} = 50$ and $k_{\bar{\theta},D} = 20$. To solve the controllability issues in (40) we take $\varepsilon = 0.1$. The desired path is designed as a slope, and an initial CM position error from the path $\big(\tilde{p}_x(0), \tilde{p}_y(0)\big) = (3\text{m}, 2\text{m})$ is considered. The path coordinates in (x, y) plane are described by

$$p_{xd} = \frac{1}{\kappa_1}\gamma, \;\; p_{yd} = \frac{1}{\kappa_2}\gamma$$

where γ is the path variable, and κ_1 and κ_2 define the path slope w.r.t. the (x, y) axes, respectively. In the simulations we take $\kappa_1 = -1$ and $\kappa_2 = 2$.

For deriving $\dot{\theta}_d$, $\ddot{\theta}_d$, $\dot{\phi}_{0_{\text{new}}}$ and $\ddot{\phi}_{0_{\text{new}}}$, we use the low-pass filtering of θ_d and $\phi_{0_{\text{new}}}$ defined in (57) and (40), respec-

tively, with the low-pass filter that has the form [Liljebäck *et al.* (2012)]

$$\dot{\Omega}_f = \begin{bmatrix} 0 & 1 \\ -\omega_n^2 & -2\zeta\omega_n \end{bmatrix} \Omega_f + \begin{bmatrix} 0 \\ \omega_n^2 \end{bmatrix} U$$

with the design parameters including natural frequency $\omega_n = 0.08$, damping ratio $\zeta = 0.07$, and initial conditions $\Omega_f(0) = [\theta_d(0), 0]^{\mathrm{T}}$ or $\Omega_f(0) = [\phi_{0_{\mathrm{new}}}(0), 0]^{\mathrm{T}}$. The simulation results are presented in the figures below.

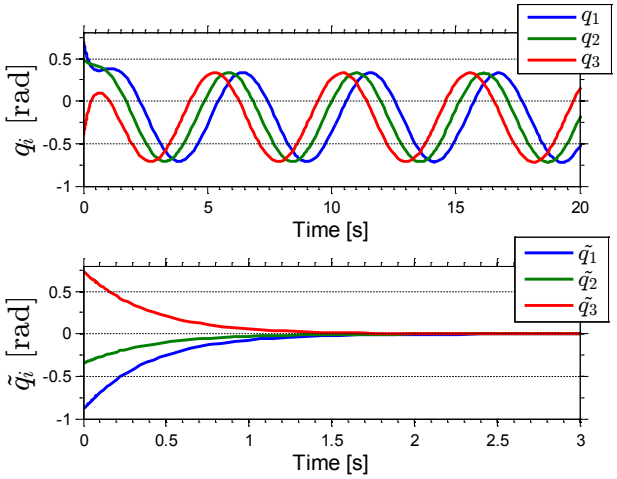

Fig. 3. Joints of the robot track the serpenoid curve (up), exponential stability of the tracking errors (down)

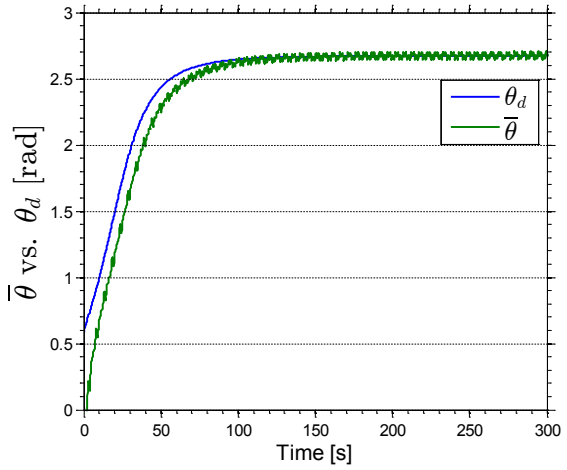

Fig. 4. Heading angle (green) tracks the desired heading angle (blue)

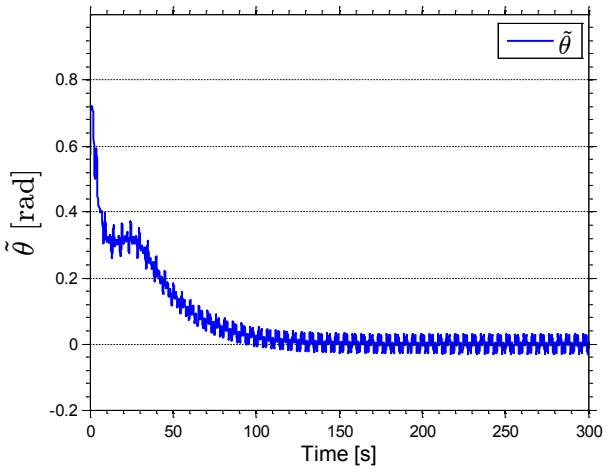

Fig. 5. Heading tracking error exponentially converges to a neighborhood of zero

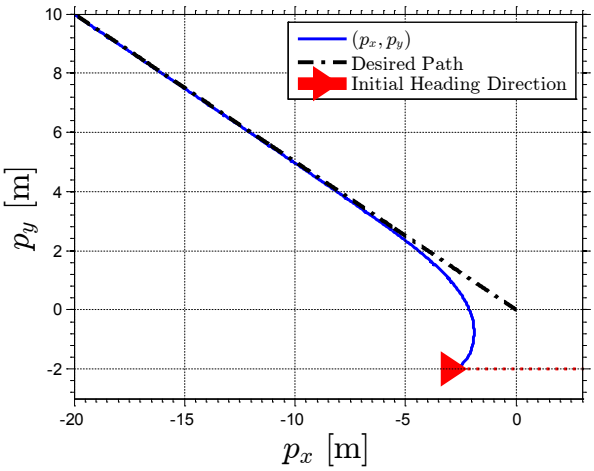

Fig. 6. The position of the CM (blue) exponentially converges to a neighborhood of the desired path (dash-dotted black)

9. CONCLUSION

We considered an analytical solution for the problem of path following control of a planar snake robot. We presented a complete model of a snake robot without velocity constraints, and based on geometric methods we analyzed the possibility of reorienting the robot in the absence of the drift term in angular part of the equations of motion. An exponentially stabilizing joint control law for the snake robot was presented. We analytically proposed a guidance-based path following control strategy for the snake robot and we showed the efficiency of our design with simulations.

REFERENCES

Bullo, F., Lewis, A., (2005). *Geometric Control of Mechanical Systems*, Springer.

Date, H., Sampei, M., Nakamura, S., (2001). Control of a snake robot in consideration of constraint force," in *Proc. IEEE Int. Conf. Control Applications*, pp. 966–971.

Gray, J., (1946). The mechanism of locomotion in snakes, *J. Exp. Biol.*, vol, 23, no.2, pp.101 - 120.

Hirose, S., (1993), *Biologically Inspired Robots*: *Snake-Like Locomotors and Manipulators,* Oxford University Press.

Khalil, H. K., (2002). *Nonlinear Systems*. Third ed., Englewood cliffs, NJ: Prentice-Hall.

Lewis, A. D., (2007). Is it worth learning differential geometric methods for modelling and control of mechanical systems?, *Robotica* 20(6), 765–777.

Liljebäck, P., Haugstuen, I. U., Pettersen, K. Y., (2010), Path Following Control of Planar Snake Robots Using a Cascaded Approach, in *Proc, IEEE Conf, Decision and Control,* Atlanta, GA, USA.

Liljebäck, P., Pettersen, K. Y., Stavdahl, Ø., Gravdahl, J. T., (2012), *Snake Robots - Modelling, Mechatronics, and Control*, ser. Advances in Industrial Control. Springer.

Ma, S., (2001). Analysis of creeping locomotion of a snake-like robot, *Adv. Robotics*, vol. 15, no. 2, pp. 205–224.

Nilsson, M., (2004). Serpentine locomotion on surfaces with uniform friction, in *Proc. IEEE/RSJ Int. Conf. Intelligent Robots and Systems*, pp.1751–1755.

Osterowski, J., Burdick, J., (1996). The geometric mechanics of Undulatory Robotic Locomotion, *International Journal of Robotics Research*.

Saito, M., Fukaya, M., and Iwasaki, T., (2002), Serpentine locomotion with robotic snakes, *IEEE Control Syst. Mag.*, vol. 22, no. 1, pp.64 - 81.

Spong, M., (1994), Partial Feedback Linearization of Underactuated Mechanical Systems, in *Proc. Intern. Conf. Intelligent Robots & Sys tems,* pp.314-321, Munich, Germany.

Transeth, A. A., Leine, R. I., Glocker, C., Pettersen, K. Y., and Liljebäck, P., (2008), Snake robot obstacle aided locomotion: Modeling, simulations, and experiments, *IEEE Transactions on Robotics*, vol. 24, no. 1, pp.88-104.